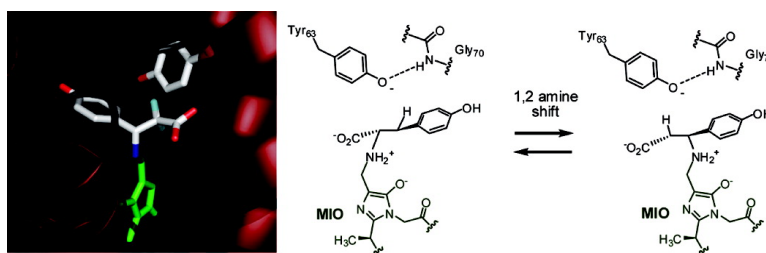


Communication

**The Mechanism of MIO-Based Aminomutases in  $\beta$ -Amino Acid Biosynthesis**

Carl V. Christianson, Timothy J. Montavon, Grace M. Festin, Heather A. Cooke, Ben Shen, and Steven D. Bruner  
*J. Am. Chem. Soc.*, **2007**, 129 (51), 15744-15745 • DOI: 10.1021/ja0762689  
 Downloaded from <http://pubs.acs.org> on February 9, 2009



**More About This Article**

Additional resources and features associated with this article are available within the HTML version:

- Supporting Information
- Links to the 1 articles that cite this article, as of the time of this article download
- Access to high resolution figures
- Links to articles and content related to this article
- Copyright permission to reproduce figures and/or text from this article

[View the Full Text HTML](#)

## The Mechanism of MIO-Based Aminomutases in $\beta$ -Amino Acid Biosynthesis

Carl V. Christianson,<sup>†</sup> Timothy J. Montavon,<sup>†</sup> Grace M. Festin,<sup>†</sup> Heather A. Cooke,<sup>†</sup>  
Ben Shen,<sup>‡,§,||</sup> and Steven D. Bruner<sup>\*†</sup>

Department of Chemistry, Merkert Chemistry Center, Boston College, Chestnut Hill, Massachusetts 02467,  
Department of Chemistry, Division of Pharmaceutical Sciences, and University of Wisconsin National Cooperative  
Drug Discovery Group, University of Wisconsin—Madison, Madison, Wisconsin 53705

Received August 20, 2007; E-mail: bruner@bc.edu

$\beta$ -Amino acids are important building blocks in a variety of polymers and small molecules. 2,3-Aminomutases catalyze the direct conversion of proteinogenic  $\alpha$ -amino acids to  $\beta$ -amino acids.<sup>1</sup> A subset of this enzyme class is dependent on the uncommon cofactor 4-methylideneimidazole-5-one (MIO) and utilizes aromatic  $\alpha$ -amino acids as substrates.<sup>2</sup> Natural product biosynthetic pathways for enediynes, taxanes, and nonribosomal peptides contain MIO-based aminomutases.<sup>2a,3</sup> The X-ray structure of tyrosine aminomutase from the enediyne C-1027 producer *Streptomyces globisporus* (SgTAM) has recently been determined.<sup>4</sup> The results established that MIO-based aminomutases are structural homologues to ammonia lyases. The mechanism of MIO-based ammonia lyases has been extensively studied; however, the role of the cofactor in the chemistry is actively debated, and not entirely resolved.<sup>5</sup> In general, two mechanisms have been proposed for MIO-catalyzed elimination of ammonia in  $\alpha$ -amino acids. The primary obstacle the enzyme overcomes is removal of a relatively nonacidic  $\beta$ -hydrogen. The highly electrophilic cofactor has been postulated to react either with the  $\alpha$ -amino group (path a) or the aromatic ring (path b) to generate the two covalent adducts shown in Figure 1 (1 or 4). Both pathways lead to deprotonation and elimination (2 or 6) of ammonia to form the conjugated olefin. On the basis of the high structural homology, the mechanism of aminomutases is likely an extension of the lyase chemistry with readdition of the amine via 1,4-conjugate addition.<sup>2,4</sup> Supporting this mechanism, aminomutase activity has been determined to proceed through a cinnamate intermediate and is reversible.<sup>2b</sup>

Any potential 2,3-aminomutase mechanism will proceed through abstraction of the  $\alpha$ - and  $\beta$ -hydrogens. To generate a stable mechanistic probe for SgTAM, we exploited  $\beta$ -Tyr analogues with fluorine atoms substituted for the  $\alpha$ -hydrogens.  $\alpha,\alpha$ -Difluoro- $\beta$ -tyrosine **11** provides an informative trapped mechanistic probe for either of the two mechanistic scenarios. The analogue was synthesized using chiral sulfinimine auxiliary chemistry starting from TBS-protected 4-hydroxybenzaldehyde.<sup>6</sup> To assess the capacity of **11** to inhibit SgTAM, an HPLC-based assay was used to determine the IC<sub>50</sub>.<sup>2</sup> The results show enzyme inhibition in a concentration-dependent manner with an IC<sub>50</sub> of 970  $\mu$ M (Figure 2B).

Cocrystals of **11** and SgTAM were prepared by incubation of the analogue with the enzyme for 1 h at room temperature followed by crystallization under conditions similar to those reported for the apo-structure.<sup>4</sup> The cocomplex structure was solved using molecular replacement and refined to 2.0 Å resolution. Overall the structure was very similar to the unliganded enzyme, with no significant

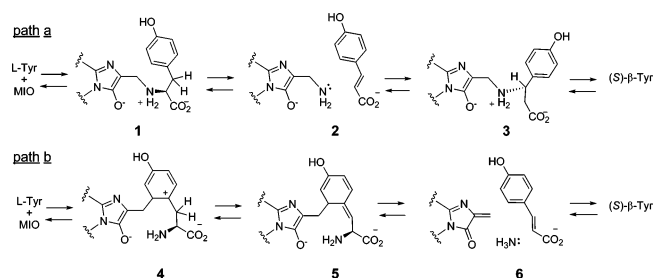


Figure 1. Mechanistic proposals for MIO-based enzymes.

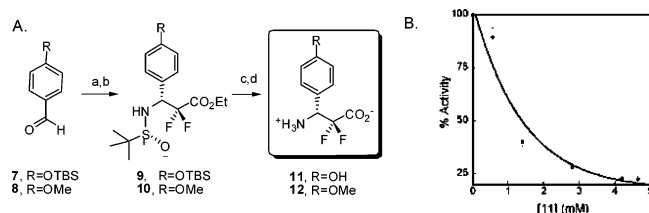


Figure 2. (A) Synthesis and evaluation of SgTAM mechanistic probes: (a) (*R*)-*tert*-butylsulfinimine, CsCO<sub>3</sub>, DCM; (b) Zn<sup>0</sup>, ethyl bromodifluoroacetate, THF; (c) 6N HCl,  $\Delta$ ; (d) *i*-PrOH, propylene oxide. (B) Concentration-dependent inhibition of SgTAM by **11**.

structural variations (rmsd over all atoms = 0.71 Å). Electron density corresponding to **11** is evident in the active site with density continuous with the MIO cofactor (Figure 3A). Multiple conformations and binding possibilities for the inhibitor were evaluated, focusing on adducts predicted by the two mechanisms shown in Figure 1. Only the amine-bound adduct (corresponding to path a) fit the density and the resulting bound-amine complex was fully refined using simulated annealing and energy minimization. The observed density does not match an MIO/phenyl ring adduct consistent with a Friedel–Crafts mechanism, and the final model places the MIO methylene carbon 3.4 Å from the *meta*-carbon of the tyrosine ring. In addition, the observed binding mode is consistent with the structure of an amino/phosphonate inhibitor bound to tyrosine ammonia lyase.<sup>7</sup> To further confirm the position of **11** in the active site,  $\alpha,\alpha$ -difluoro- $\beta$ -4-methoxyphenylalanine **12** was prepared and crystallized with SgTAM. By applying the diffraction data from the cocomplex of **12** to the isomorphous structure of **11**-bound, electron density corresponding to the variant methoxy group is easily observed. As shown in Figure 3C, the difference map ( $F_o - F_c$ ) of the methoxy adduct establishes the position of the methyl group in **12** as consistent with our structural assignment of the bound inhibitor. The methyl group is accommodated in the active site by displacing an ordered water molecule (Figure 3A).

The cocrystal structure of **11**/SgTAM provides detailed insight into the chemistry of the reversible 1,2 amino shift catalyzed by SgTAM. The key substrate specificity determinants for the amino

<sup>†</sup> Boston College.

<sup>‡</sup> Department of Chemistry, University of Wisconsin.

<sup>§</sup> Division of Pharmaceutical Sciences, University of Wisconsin.

<sup>||</sup> University of Wisconsin National Cooperative Drug Discovery Group, University of Wisconsin.

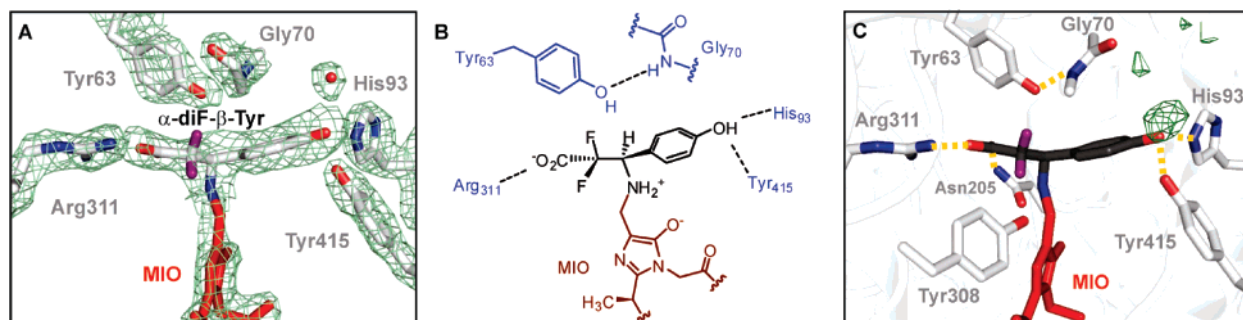


**Figure 3.** Structure of *SgTAM* bound to the substrate analogue **11**. (A) Electron density map ( $2F_o - F_c$  at  $1.5\sigma$ ) showing the active-site region. The inhibitor is shown in black and the MIO cofactor red. (B) Representation of the major interactions and conformation of the enzyme with the bound analogue. (C) View of the active site showing the electron density map ( $F_o - F_c$  at  $2.0\sigma$ ) calculated from cocrystals of analogue **12** showing the position of the methyl group.

acid are His93 and Tyr415. These two residues form a bifurcated hydrogen bond with the substrate phenol (Figure 3AB). The residue corresponding to His93 has been implicated as a key specificity determinant in tyrosine and phenylalanine ammonia lyases.<sup>7,8</sup> The carboxylate of the amino acid forms hydrogen bonds with Arg311 and Asn205. Overall, the active site contains a high percentage of aromatic residues. The MIO is stacked with Phe356 (not illustrated) and Tyr308 is adjacent to the methylene of the MIO. Tyr63 is positioned in close proximity to the  $\alpha$  and  $\beta$ -carbons of the inhibitor and is well-positioned to assist in the elimination chemistry. Gly70 forms a hydrogen bond with the phenol of Tyr63 and both residues are conserved in all MIO-based lyases and mutases. Tyr63 and Gly70 reside on a loop that is often disordered in unliganded ammonia lyase crystal structures. The phenolic oxygen of Tyr63 is positioned 3.2 Å away from the  $\alpha$ -carbon and 3.4 Å from the  $\beta$ -carbon of the bound inhibitor. Tyr63, in the phenolate state, can act as a general base (Figure 4), shuttling the proton between the  $\alpha$ - and  $\beta$ -positions. The  $pK_a$  of Tyr63 needs to be lowered in the active site of *SgTAM* to favor the anionic form. Two aspects are evident from the structure that contribute to a lower  $pK_a$ : (i) stabilization of the negative charge by the backbone hydrogen bond of Gly70 and (ii) the significant number of  $\alpha$ -helices with positive dipoles pointed at the active site both will favor the phenolate. Also consistent with this mechanism, the measured optimal pH for *SgTAM* is  $\sim 9$ .<sup>2b</sup> To confirm the importance of Tyr63 in the reaction mechanism, site-directed mutagenesis was used to remove the phenol by substituting phenylalanine. The resulting mutant, Tyr63Phe, had no measurable aminomutase activity up to 1.9 mM substrate concentration (see Supporting Information).

The reaction of the related phenylalanine aminomutase has been shown to proceed through stereospecific exchange of the *proS* hydrogen.<sup>9</sup>  $\alpha$ -Tyr bound to MIO in a *trans*-configuration places the *proS* hydrogen in proximity to Tyr63 and anti-periplanar to the ammonium leaving group. The stereochemistry of the reverse reaction of aminomutases ( $\beta$ -Tyr to  $\alpha$ -Tyr) is variable. *SgTAM* catalyzes the racemization of (*S*)- $\beta$ -Tyr and a highly homologous tyrosine aminomutase from chondramide biosynthesis produces the opposite stereochemistry at the  $\beta$ -position, (*R*)- $\beta$ -Tyr.<sup>3c</sup> The stereochemical differentiation can occur from rotation of the *trans*-cinnamate intermediate to present the opposite face to the amine-

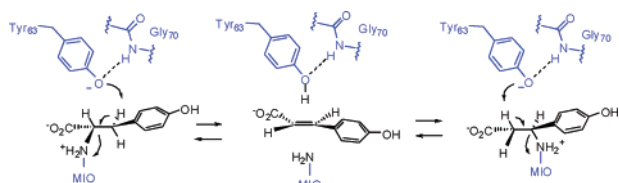


**Figure 4.** Proposed mechanism for *SgTAM* activity.

MIO adduct. Modeling of this orientation shows the active site can accommodate this change while still maintaining binding interactions between Arg311, His93, and Tyr415.

The presented structures of the aminomutase *SgTAM* provide strong evidence that MIO-based enzymes use covalent catalysis through the  $\alpha$ -amine to direct the chemistry. For ammonia lyases, a covalent adduct orients both an enzymatic base and the leaving group for an  $E_2$ -type elimination. For enzymes with aminomutase activity, the conjugate 1,4-addition into the relatively nonelectrophilic 4-hydroxycinnamate is facilitated by orienting the amino-bound intermediate and maintaining the nucleophile in the neutral form. Differentiation of the two catalytic pathways can be accomplished by retention of ammonia in the closed active site of aminomutases.<sup>4</sup>

**Acknowledgment.** This work is supported in part by funds from Boston College and the Damon Runyon Cancer Research Foundation DRS-41-01 (S.D.B.) and NIH Grants CA78747 and CA113297 (B.S.). We thank Dr. Y. Li, Institute of Medicinal Biotechnology, Chinese Academy of Medical Sciences, Beijing, China, for the C-1027-producing *S. globisporus* strain and A. Orville and the staff at the Brookhaven NSLS PXR for assistance with X-ray data collection.

**Supporting Information Available:** Full experimental details for synthesis and characterization of inhibitors, co-complex crystallization, structure determination and biochemical characterization of inhibitors/mutant enzymes. This material is available free of charge via the Internet at <http://pubs.acs.org>.

## References

- (a) Wetmore, S. D.; Smith, D. M.; Radom, L. *J. Am. Chem. Soc.* **2001**, *123*, 8678–8689. (b) Lelais, G.; Seebach, D. *Biopolymers* **2004**, *76*, 206–243.
- (a) Christenson, S. D.; Liu, W.; Toney, M. D.; Shen, B. *J. Am. Chem. Soc.* **2003**, *125*, 6062–6063. (b) Christenson, S. D.; Wu, W.; Spies, M. A.; Shen, B.; Toney, M. D. *Biochemistry* **2003**, *42*, 12708–12718.
- (a) Walker, K. D.; Klettke, K.; Akiyama, T.; Croteau, R. *J. Biol. Chem.* **2004**, *279*, 53947–53954. (b) Jin, M.; Fischbach, M. A.; Clardy, J. *J. Am. Chem. Soc.* **2006**, *128*, 10660–10661. (c) Rachid, S.; Krug, D.; Weissman, K. J.; Müller, R. *J. Biol. Chem.* **2007**, *282*, 21810–21817.
- Christianson, C. V.; Montavon, T. J.; Van Lanen, S. G.; Shen, B.; Bruner, S. D. *Biochemistry* **2007**, *46*, 7205–7214.
- (a) Poppe, L.; Retey, J. *Angew. Chem., Int. Ed. Engl.* **2005**, *44*, 3668–3688. (b) Hermes, J. D.; Weiss, P. M.; Cleland, W. W. *Biochemistry*, **1985**, *24*, 2959–2967.
- (a) Staas, D. D.; Savage, K. L.; Homnick, C. F.; Tsou, N. N.; Ball, R. G. *J. Org. Chem.*, **2002**, *67*, 8276–8279. (b) Sorochinsky, A.; Voloshin, N.; Markovsky, A.; Belik, M.; Yasuda, N.; Uekusa, H.; Ono, T.; Berbasov, D. O.; Soloshonok, V. A. *J. Org. Chem.* **2003**, *68*, 7448–7454.
- Louie, G. V.; Bowman, M. E.; Moffitt, M. C.; Baiga, T. J.; Moore, B. S.; Noel, J. P. *Chem. Biol.* **2006**, *13*, 1327–1338.
- Watts, K. T.; Mijts, B. N.; Lee, P. C.; Manning, A. J.; Schmidt-Dannert, C. *Chem. Biol.* **2006**, *13*, 1317–1326.
- Mutatu, W.; Klettke, K. L.; Foster, C.; Walker, K. D. *Biochemistry* **2007**, *46*, 9785–9794.

JA0762689